Indian Geotechnical Journal, 41(3), 2011, 131-142

Reliability analysis of shallow landslides under seismic loading

Sanjay K. Jha[1]

Key words

Critical seismic coefficient, first order reliability method, Monte Carlo simulation, Newmark sliding block method, point estimate method.

Abstract: Shallow landslides are often analyzed using infinite slope stability method. In infinite slope stability method, the pseudo-static safety factor of the slope is dependent on the inertial effects and on the reduction of shear strength induced in the soil mass by the seismic loading. The Newmark block model is commonly used to predict slope displacements under seismic loading. In using the Newmark model, inertial force is assumed to be either parallel to the slope or horizontal which may overestimate the critical seismic coefficient, an important parameter for safety and displacement analysis of the slope. An approach is discussed here to determine the minimum critical seismic coefficient for infinite slopes. Probabilistic methods are applied to model and analyze the relevant sources of uncertainty involved in stability analysis of shallow landslides. Four different methods: a first order second moment (FOSM) method, an advanced first order second moment (AFOSM, Hasofer Lind) method, a point estimate method (PEM), and a Monte Carlo simulation method (MCSM) are used to quantify the uncertainty in the calculated reliability index. An exampie is presented to investigate how the probability of failure or the reliability index may vary among these four methods. Also the effects of variability of the critical seismic coefficient on the permanent deformation of the slope are discussed.

Introduction

Natural soil properties vary considerably, even within uniform soil layers. Most soil parameters within the domain of analysis of geotechnical work have some sort of variability. Inherent variability, measurement error and transformation uncertainty are the three primary sources of geotechnical variability (Phoon and Kulhawy 1999). Missing geological details during the exploration program, estimation of soil properties that are difficult to quantify, i.e., the spatial variability of soil properties in the field, fluctuation in pore water pressure and testing errors as well as many other relevant factors are encountered during slope stability computations (Malkawi et al. 2000). In a deterministic analysis, the safety of the slope is defined based on a safety factor (F), defined as the ratio of resisting to driving forces on a potential sliding surface. The slope is considered safe if the calculated safety factor is greater than one. Due to the uncertainty in material properties as well as model error and random processes such as an earthquake event, the parameters required to calculate the safety factor cannot be defined as deterministic values and even a safety factor greater than one does not confirm the stability of the concerned slope. In a probabilistic approach, the factor of safety is expressed in terms of its mean value and its variance. Reliability analysis can therefore be used to assess uncertainties in engineering variables such as the slope safety factor in terms of reliability index (β) (Malkawi et al. 2000).

Shallow landslides are often analyzed using infinite slope stability method (Wang and Lin 2010). In infinite slopes analyses, the pseudo-static (dynamic) safety factor of the slope is dependent on the inertial effects and on the reduction of shear strength induced in the soil mass by the seismic loading. In this regard, the sliding block model introduced by Newmark (1965) can be suitably used for the prediction of permanent displacements, with uncertainties that are usually associated with the choice of the design seismic motion. In infinite slopes, weakening instabilities may occur due to excess pore pressure build-up that may lead to liquefaction, possibly causing a local or even global failure of the slope. Biondi et al. (2000, 2002) proposed a procedure to evaluate the seismic stability and the displacement response of slopes accounting for shear strength reduction due to excess pore pressure developed during seismic events.

Newmark sliding block analyses have been frequently used to calculate the permanent displacement of the slope. While calculating the permanent displacement of the slope, it involves integration of an input motion relative to yield acceleration, and thus the manner in which the yield acceleration is determined is important (Kramer and Lindwall 2004). In using the Newmark model, inertial force is generally assumed to be either horizontal or parallel to the slope, which may overestimate the critical seismic coefficient, an important parameter for

1 Former graduate student, Department of Civil and Environmental Engineering, Saitama University, Japan, Email: ersanjaynp@gmail.com

displacement analysis of the slope. Original Newmark analyses use inertial force parallel to the failure surface, whereas Kramer (1996); Makdisi and Seed (1978); Seed and Goodman (1964) among others used a horizontal inertial force, and thus the assumption of seismic force direction is unclear. An approach is presented in this paper to determine the minimum critical seismic coefficient for infinite slopes.

A number of researchers have done probabilistic stability analyses of the slope safety factor using different approaches. Al-Homoud and Tahtamoni (2000) used a first order second moment (FOSM) method to study the statistics of earthquake induced displacements for 3D slopes. Hassan and Wolff (2000) used the FOSM method, the advanced first order second moment (AFOSM or Hasofer Lind) method and the point estimate method (PEM) for analyzing slope reliability. Malkawi et al. (2000), Hata et al. (2008) used Monte Carlo simulation method (MCSM) for slope reliability analysis. Similar probabilistic stability analyses of slopes based on the finite element method have been done, for example, by Xu and Low (2006), among others.

In the analysis of shallow landslides using infinite slope approach, besides the uncertainties in soil properties (e.g. unit weight, cohesion, friction angle), uncertainties in seismic design motion and excess pore pressure (for saturated cohesionless soils) developed during seismic event may affect the slope reliability. The effect of uncertainties in seismic design motion and excess pore pressure developed during seismic events on reliability index of infinite slopes are investigated in this study using four probabilistic methods: FOSM method, AFOSM or Hasofer Lind (HL) method, PEM and MCSM. An example is presented to investigate how the reliability index of infinite slopes may vary among these four methods. Also the effect of variability of the critical seismic coefficient on the permanent deformation of the slope is evaluated.

Deterministic Analysis of an Infinite Slope

Figure 1 shows an infinite slope with an inclination α, driven by a seismic force directed towards an angle θ with the slope. The infinite slope is assumed to have a phreatic surface between the ground surface and the potential sliding surface. The initial total normal stress, σ_0 and initial driving shear stress, τ_0 on the sliding surface, corresponding to the static conditions prior to the earthquake, can be derived from the normal and tangential components of weight, W, of a soil column of width b =1 with respect to the direction of slip surface as follows:

$$\sigma_0 = \gamma H \cos^2 \alpha \qquad (1a)$$

$$\tau_0 = \gamma H \sin\alpha \cos\alpha \qquad (1b)$$

where H is the height of the soil mass above the sliding surface, and γ is the average unit weight of the soil within the sliding mass. The initial pore-water pressure, u_0 on the slip surface due to a height H_w of the phreatic surface is:

$$u_0 = \gamma_w H_w \cos^2 \alpha = mH\gamma_w \cos^2 \alpha \qquad (2)$$

where γ_w is the unit weight of water (taken here as 10 KN/m³) and $m = H_w/H$

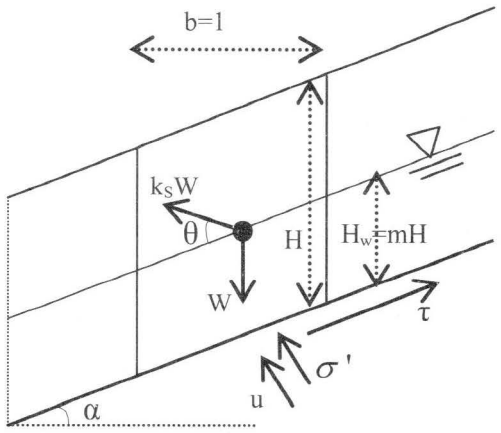

Fig. 1 Stress state of an infinite slope

Using the Mohr-Coulomb failure criterion, the infinite slope static safety factor can be expressed in the form:

$$F_s = \frac{\tau_{f0}}{\tau_0} = \frac{\tan\phi'}{\tan\alpha}\left(1 - \frac{\gamma_w}{\gamma} m\right) \qquad (3)$$

where ϕ' is the angle of shearing resistance of the soil.

The seismic components of the total normal stress, $\Delta\sigma$, and the driving shear stress, $\Delta\tau_d$, on the sliding surface due to the inertial force imposed by the earthquake loading on the slope (Figure 1) can be expressed as:

$$\Delta\sigma = k_s \gamma H \sin\theta \cos\alpha \qquad (4a)$$

$$\Delta\tau_d = k_s \gamma H \cos\theta \cos\alpha \qquad (4b)$$

where k_s is the seismic coefficient of earthquake acceleration, $k_s = a_s/g$ (a_s is the seismic acceleration and g is the acceleration due to gravity).

For a seismic force driving the slope downward, the dynamic total normal stress σ, driving shear stress τ_d, and pore pressure u, on the sliding surface at a certain instant during an earthquake will be given by following Eqs:

$$\sigma = \sigma_0 - \Delta\sigma \tag{5a}$$

$$\tau = \tau_0 + \Delta\tau_d \tag{5b}$$

$$u = u_0 + \Delta u = u_0 + r_u\sigma_0' \tag{5c}$$

where r_u is the excess pore pressure ratio ($\Delta u / \sigma_0'$).

The pseudo-static seismic safety factor (F_d) of the infinite slope is:

$$F_d = \frac{\left[(1-\frac{\gamma_w}{\gamma}m)(1-r_u)\cos\alpha - k_s\sin\theta\right]\tan\phi'}{(\sin\alpha + k_s\cos\theta)} \tag{6}$$

It is apparent that during a seismic event the reduction in the pseudo-static safety factor depends on the inertial effect as well as on the pore pressure increment induced by the seismic loading. Figure 2 shows the variation of the pseudo-static safety factor versus the earthquake induced acceleration coefficient k_s. Curves are given for two different values of earthquake induced pore pressure ratio r_u. If seismic shaking does not induce significant pore pressure or if the excess pore pressure generated is ignored ($r_u = 0$), the pseudo-static safety factor is given by:

$$F_{d0} = \frac{\left[(1-\frac{\gamma_w}{\gamma}m)\cos\alpha - k_s\sin\theta\right]\tan\phi'}{(\sin\alpha + k_s\cos\theta)} \tag{7}$$

According to the sliding block model proposed by Newmark, the potential sliding mass is treated as a rigid body and permanent displacements occur whenever the ground acceleration exceeds the critical value. The critical seismic coefficient k_c refers to the seismic coefficient corresponding to $F_d = 1$ and thus can be obtained from Eq. 6 as:

$$k_c = \frac{(1-\frac{\gamma_W}{\gamma}m)(1-r_u)\cos\alpha\tan\phi' - \sin\alpha}{(\cos\theta + \sin\theta\tan\phi')} \tag{8}$$

This critical seismic coefficient is not constant but varies with time during earthquake shaking depending on r_u (Biondi et al. 2000, 2002). The initial value of the seismic coefficient when $r_u = 0$ is given by:

$$k_{c0} = \frac{(1-\frac{\gamma_W}{\gamma}m)\cos\alpha\tan\phi' - \sin\alpha}{(\cos\theta + \sin\theta\tan\phi')} \tag{9}$$

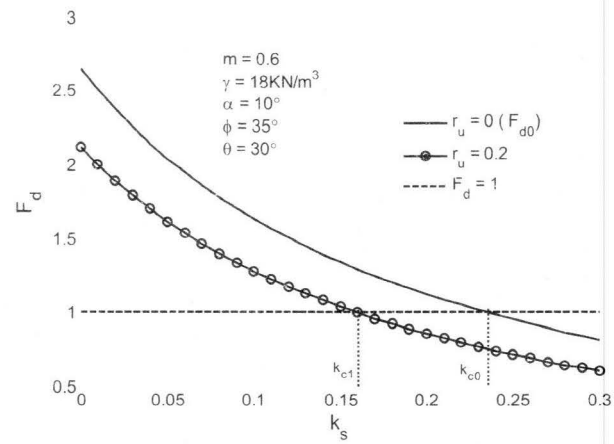

Fig. 2 Variation of pseudo-static safety factor with seismic coefficient

If ground acceleration exceeds the critical acceleration, permanent displacements occur in the slope and thus determination of critical seismic coefficient is considered important. As shown in Eq. 8, for known slope properties, the critical seismic coefficient is dependent on the seismic force inclination θ. Original Newmark analyses assume k_s is parallel to the failure surface (i.e., $\theta = 0$ in Figure1) and is given by:

$$k_c = (1-\frac{\gamma_W}{\gamma}m)(1-r_u)\cos\alpha\tan\phi' - \sin\alpha \tag{10}$$

which ultimately simplifies to: $k_c = \cos\alpha\tan\phi' - \sin\alpha$, for a dry infinite slope as derived by Newmark.

Kramer (1996); Makdisi and Seed (1978); Seed and Goodman (1964); Hata et al. (2008) used k_s as horizontal ($\theta = \alpha$ in Figure 1) to calculate inertial forces. For dry infinite slopes, this is given by substituting $\theta = \alpha$ in Eq. 8 and results in $k_c = \tan(\phi' - \alpha)$. According to Kramer and Lindwall (2004), for a 2:1 (H: V, α = 26.6°) infinite slope with ϕ' =35°, the yield seismic coefficient ($k_y = k_c$) =0.178; when the inertial force acts parallel to the slope, k_y =0.148; when the inertial force is horizontal, k_y =0.146, a minimum value, when

the inertial force is at its critical angle of 8.5° inclined from horizontal. They also suggested that stability is not very sensitive to inertial force inclination, and that the assumption of a horizontal inertial force provides a good approximation to the critical case. However, a considerable difference may occur depending on the slope geometry and soil parameters. For example if α=10° and ϕ'=35°: k_y = 0.515 when the inertial force acts parallel to the slope, k_y=0.466 when the inertial force is horizontal, and k_y=0.422 when the inertial force is at its critical angle of 35° inclined from the slope (or 25° with the horizontal). Thus to obtain the minimum critical yield acceleration, it is necessary to determine the inclination of the inertial force. To obtain the critical seismic coefficient inclination, Eq. 8 is minimized with respect to θ such that:

$$\frac{\partial k_C}{\partial \theta} = 0 \qquad (11)$$

By solving Eq. 11, it is found that k_c will be a minimum when $\theta = \phi'$. This is also valid for the two examples presented earlier and thus it can be concluded that neither the horizontal nor parallel to the slope assumption of inclination of the inertial force produces the minimum critical seismic coefficient. Inclination of inertial force at an angle ϕ' to the slope or at an angle $\phi'-\alpha$ to the horizontal produces the minimum critical seismic coefficient given by:

$$k_c = (1-\frac{\gamma_W}{\gamma}m)(1-r_u)\cos\alpha\sin\phi' - \sin\alpha\cos\phi' \qquad (12)$$

If the actual seismic coefficient during an earthquake is larger than the critical seismic coefficient, a permanent displacement will occur and thus the minimum value of the critical seismic coefficient obtained using Eq. 12 should be used for infinite slope stability analysis. A displacement analysis can be carried out based on the sliding block model by double integration of the following equation of motion:

$$a(t) = [k(t) - k_c(t)]g \qquad (13)$$

where $a(t)$ is the relative acceleration of the slope, $k(t)$ and $k_c(t)$ are the current and critical seismic coefficients, respectively. The critical seismic coefficient depends on slope and soil conditions and also on excess pore pressure developed at a certain instant. As the excess pore pressure during a seismic event increases with time, the critical seismic coefficient decreases and an initially stable slope may fail after an increase in excess pore pressure and complete liquefaction of the slope may occur after any further increases in excess pore pressure. For displacement calculation using the Newmark method, the horizontal component of critical seismic coefficient is required (Ingles et al. 2006), and given by $k_{ch} = k_c\cos(\phi'-\alpha)$. Considering the effect of both the horizontal and vertical component of the critical seismic coefficient, Ingles et al. (2006) expressed the following equation for cohesionless soils for downhill motion:

$$k_{ch} = \frac{\cos\alpha\tan\phi' - \sin\alpha - m\frac{\gamma_w}{\gamma}\cos\alpha\tan\phi'}{k_1(\cos\alpha\tan\phi' - \sin\alpha) + (\sin\alpha\tan\phi' + \cos\alpha)} \qquad (14)$$

where $k_1 = k_{sv}/k_{sh} = \tan(\theta-\alpha)$; k_{sv} and k_{sh} are the horizontal and vertical components of k_s. Substituting the value of k_1, using $k_c = k_{ch}/\cos(\theta-\alpha)$ and differentiating Eq. 14 with respect to θ such that $\partial k_c/\partial\theta = 0$, results $\theta = \phi'$. Thus, the inclination of the inertial force should be taken as that of the angle of internal shear resistance, ϕ' of the soil with the slope. The variation of k_c with inertial force inclination for different values of m and r_u is shown in Figure 3.

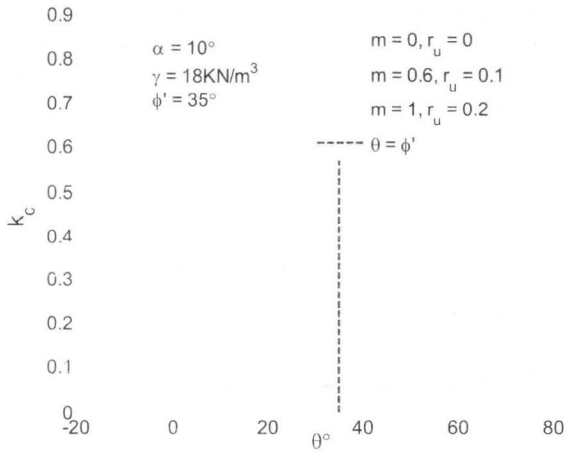

Fig. 3 Variation of critical seismic coefficient with angle of inclination of seismic force with slope

The critical seismic coefficient can also be used to define the alternative pseudo-static safety factor F_k (Baker et al. 2006) as:

$$F_k = \frac{k_c}{k} \qquad (15)$$

where k is the expected magnitude of the pseudo-static coefficient at a particular site.

The value of k depends on the seismological information such as earthquake magnitude, focal distance, etc. Baker et al. (2006) proposed an empirical relationship to calculate k_c for cohesionless dry infinite slopes ($m = 0, r_u = 0$) as:

$$k_c \approx \frac{\phi' - \alpha}{56.5} \tag{16}$$

where ϕ' and α are expressed in degrees or if expressed in radians, $k_c \approx \phi' - \alpha$. As stated earlier, $k_c = \sin(\phi' - \alpha)$ is obtained for similar conditions using Eq. 12. Eq. 16 produces only 0 to 4.7% higher values of k_c than that computed from Eq. 12 depending on value of $\phi' - \alpha$ from 0 to 30° and thus both approaches gives a similar value of k_c.

For a given seismic coefficient less than the critical value, a pseudo-static safety factor greater than one is obtained and if the seismic coefficient is greater than the critical value, pseudo-static safety factor is less than one. The relationship between the pseudo-static safety factor and the inertial force inclination angle θ is shown in Figure 4. As shown in Figure 4, the pseudo-static safety factor is a non-linear function of θ and it attains a minimum value at a certain θ, which depends on slope properties as well as excess pore pressure developed during the seismic event.

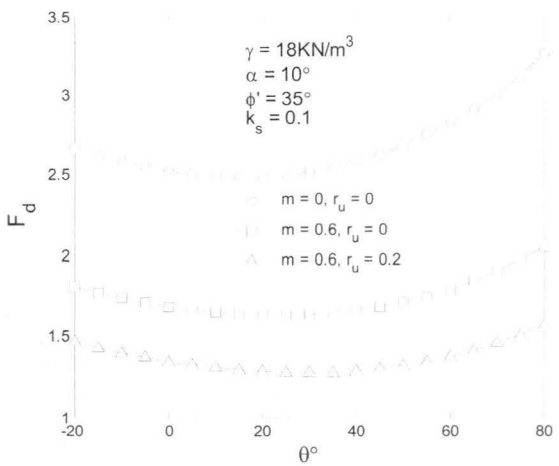

Fig. 4 Variation of pseudo-static safety factor with seismic force inclination

Reliability Approach

The safety factor calculated from the deterministic stability analysis cannot be considered as a consistent measure of risk. Due to uncertainties involved in characterizing the soil properties, and model errors associated with the analytical technique adopted, slopes with a factor of safety larger than unity still have some probability of failure. To account for these uncertainties, probabilistic stability analysis is necessary where the failure probability, p_f for the slopes can be defined as

$$p_f = P[g(X) \le 0] = \int_{G(X) \le 0} f(X)dx \tag{17}$$

where $g(X)$ = performance function and can be defined as:

$$g(X) = F(X) - 1 \tag{18}$$

where $F(X)$ = function for the factor of safety; $f(X)$ = joint probability density function of the basic variable vector **x**.

The mean and variance of the performance function can be reasonably approximated by the first order Taylor series expansion about the mean. Once the mean and variance of the performance function is obtained, the reliability index, β can be defined as:

$$\beta = \frac{\mu_g}{\sigma_g} = \frac{\mu_F - 1}{\sigma_F} \tag{19}$$

where μ_g, μ_F are the mean values of the performance function $g(X)$ and the mean value of safety factor, respectively; σ_g and σ_F are the standard deviations of performance function $g(X)$ and safety factor, respectively. Assuming that the performance function and all the random variables are normally distributed, the probability of failure can be evaluated by:

$$p_f = 1 - \Phi(\beta) \tag{20}$$

where $\Phi(.)$ is the standard normal cumulative probability.

Assuming that the safety factor follows a lognormal distribution, the reliability index, β is expressed as (Duncan 2000):

$$\beta = \frac{\ln\left[\frac{\mu_F}{\sqrt{(1+V_F^2)}}\right]}{\sqrt{\ln(1+V_F^2)}} \tag{21}$$

where V_F is the coefficient of variation of the safety factor.

There are several methods to evaluate the reliability or probability of failure of a particular slope. It should be noted that, in general, the performance function is neither a linear function nor normally distributed and it is often difficult to define the distribution of associated variables. In such situation, FOSM and AFOSM methods provide approximate results. FOSM, AFOSM and PEM can also consider the correlation between the two variables, however, the effect of correlation between the variables is not considered in this study. To consider the effects of empirical distribution of variables, correlation between the variables and correlation length, Monte Carlo simulation may provide benchmark results. In the present study, the comparison of reliability indices obtained using different methods is done assuming the random variables as normally distributed and independent.

First order second moment (FOSM) method

According to the first order Taylor series approximation with non-correlated random variables, the mean value of the pseudo-static safety factor is obtained by evaluating the function at the mean values of the random variables as:

$$\mu_{F_d} = \frac{\left[(1-\frac{\gamma_w}{\mu_\gamma} m)(1-\mu_{r_u})\cos\alpha - \mu_{k_S}\sin\mu_\theta\right]\tan\mu_{\phi'}}{(\sin\alpha + \mu_{k_S}\cos\mu_\theta)} \quad (22)$$

where $\mu_\gamma, \mu_{\phi'}, \mu_{k_S}, \mu_\theta$ and μ_{r_u} are the mean values of the unit weight of the soil within the sliding mass, angle of effective friction angle, seismic coefficient, inclination of seismic force with the slope and excess pore pressure ratio developed during the seismic event at particular instant, respectively. All the variables considered here are assumed to be uncorrelated. Similarly, the first order approximation of the variance of the pseudo-static safety factor evaluated at the mean values can be written as:

$$\mathrm{Var}(F_d) = \left(\frac{\partial F_d}{\partial \gamma}\right)^2 \mathrm{Var}(\gamma) + \left(\frac{\partial F_d}{\partial \varphi'}\right)^2 \mathrm{Var}(\varphi') + \left(\frac{\partial F_d}{\partial k_s}\right)^2 \mathrm{Var}(k_s) + \left(\frac{\partial F_d}{\partial \theta}\right)^2 \mathrm{Var}(\theta) + \left(\frac{\partial F_d}{\partial r_u}\right)^2 \mathrm{Var}(r_u) \quad (23)$$

where $\partial F_d / \partial \gamma, \partial F_d / \partial \varphi', \partial F_d / \partial k_s, \partial F_d / \partial \theta$ and $\partial F_d / \partial r_u$ are the partial derivatives of pseudo-static safety factor (Eq. 6) with respect to unit weight of the soil within the sliding mass, angle of effective friction angle, seismic coefficient, inclination of seismic force with the slope and excess pore pressure ratio, respectively evaluated at their mean values. The details of the FOSM can be found in literature (e.g. Malkawi et al. 2000).

Advanced first order second moment (Hasofer Lind) method

The second moment reliability index, β as defined by Hasofer and Lind (1974) considers the effect of both the mean values and the covariance of the random variables influencing the design. It also includes the effect of the type of probability distributions of random variables considered. The matrix formulation of the Hasofer-Lind reliability index and simplified reliability calculation is proposed by Low and Tang (1997) where the reliability index is given by:

$$\beta = \min_{x\in F} \sqrt{\left[\frac{x_i - \mu_i^N}{\sigma_i^N}\right]^T [R]^{-1} \left[\frac{x_i - \mu_i^N}{\sigma_i^N}\right]} \quad (24)$$

where x_i is a vector representing the set of random variables; μ_i^N is the equivalent normal mean value; σ_i^N is the equivalent normal standard deviation; R is the correlation matrix; and F is the failure domain. The details of the calculation procedure of β can be found in Low and Tang (1997) and Low (2005).

Point estimate method (PEM)

The point estimation method (PEM) developed by Rosenblueth (1975, 1981) provides the statistical moments (mean, variance and skewness) for the dependent variable, like the safety factor in case of slope stability analysis, when it can be expressed as a function of other random variables. The required inputs for an infinite slope stability analysis are: a) a defined performance function b) estimated value for each input attribute if it is assumed to have no or negligible variability and c) estimated mean and standard deviation of each input random variable. The mean and COV of the safety factor are calculated and assuming the safety factor follows a normal distribution, the reliability index is given by Eq. 19. Details of the calculation procedure using PEM can be found in Baecher and Christian (2003).

Monte Carlo simulation method

In Monte Carlo simulation method, the values of the random variables are generated consistent with their probability distributions and the safety factor is calculated for each generated set of variables. The process is repeated numerous times and the expected

value and the standard deviation of the function of the safety factor are calculated. The shape of the corresponding probability distribution functions can also be determined. To obtain an approximate shape of the safety factor PDF, 10^6 pairs of data were taken from the input variables and the resulting histogram and the PDF of dependent variable was plotted.

Results and Discussion

Reliability index using FOSM

Using the FOSM method explained above, the reliability index is computed using Eqs. 19, 20, 22, 23. The reliability index for a typical infinite slope with the mean and COV of variations shown in Table 1 is computed and given in Table 2 as β_{FOSM}. A reliability index β = 1.01 (probability of failure, p_f = 15.6%) is obtained for m=0.6 whereas β = 2.05 (p_f = 2%) is obtained for m=0.2. If a minimum COV (V) of variables is considered (say, $V_\gamma = 0.002$, $V_{\phi'} = 0.02$, $V_{k_s} = 0.025$, $V_\theta = 0.05$ and $V_{r_u} = 0.03$), a reliability index β = 7.4 (p_f = 6.8E-12%) is obtained for m=0.6 whereas β = 14.7 (p_f = 0%) is obtained for m=0.2. For m=0.6, the reliability index β reduces to 1.01 from 7.4 if the COVs of the input variables are assumed to be the values shown in Table 1. However, it should be noted that the reduction of the reliability index is dependent on the variability of input variables.

Comparison of reliability index using different probabilistic methods

A comparative study among FOSM, AFOSM, PEM and MCSM is presented using the soil properties and seismic parameters of Case 1. Figure 5 shows the histogram plot of the obtained pseudo-static safety factor for Case 1 for the mean and COV of variables as indicated in Table 1 along with the normal and lognormal probability density functions (PDF) of the pseudo-static safety factor using the mean and standard deviation obtained from the MCSM. It can be seen that the lognormal distribution assumption for the pseudo-static safety factor is closer to the obtained histogram than normal distribution. To obtain the pseudo-static safety factor histogram, a random value from variables as well as deterministic values of other parameters was taken to calculate the pseudo-static safety factor. All the variables are assumed to have normal distribution. For Case 1, the reliability indices using normal and lognormal distribution assumption of pseudo-static safety factor (using Eqs. 19 and 21, respectively) are 1.11 and 1.18, respectively. Similarly, for Case 2, the reliability indices using normal and lognormal distribution assumption are 2.10 and 2.71, respectively.

The effect of COV of soil and seismic parameters on reliability index using FOSM, AFOSM, PEM, and MCSM are shown in Figure 6. For variation in COV of soil unit weight, no variations were observed among FOSM, PEM and MCSM, however some difference was observed for AFOSM. The reliability index using AFOSM (Hasofer Lind reliability index) is slightly higher for $V_\gamma \leq 0.04$ and slightly lower for $V_\gamma > 0.04$. For the case of variation in $V_{\phi'}$, all the four methods produce similar results. For variation in V_{k_s} and V_θ , the Hasofer Lind reliability index is slightly higher than the other methods. Similarly, for variation in V_{r_u}, MCSM provides a lower reliability index for V_{r_u} > 0.3 and at lower variability, a slight difference in reliability index among different methods is observed. For Case 1 of typical COV of variables considered, as shown in Table 2, reliability indices of 1.01, 1.12, 1.13, and 1.11 were obtained using FOSM, AFOSM, PEM and MCSM, respectively. For Case 2, reliability indices of 2.05, 2.58, 2.14 and 2.10 were obtained using FOSM, AFOSM, PEM and MCSM, respectively. In comparison to MCSM, a difference of -9 to 2% in the reliability index is obtained for Case 1 and a difference of -2 to 23% is obtained for Case 2 using other methods.

Thus the difference in computed reliability index using FOSM, AFOSM, PEM and MCSM is dependent on the soil variability, seismic parameters variability as well as initial slope conditions. The difference in computed reliability indices may be attributed to the underlying assumption and methodology in computing reliability index. However, any method can be used for calculation of the reliability index with a good accuracy. Moreover, all these probabilistic methods consider the effect of uncertainty in soil and seismic parameters that are not accounted for in deterministic analysis. From Figure 6, it can be seen that variability in the internal friction angle is the most critical parameter followed by variability in the seismic coefficient and excess pore pressure coefficient. For example if V_{r_u} increases from 0.03 to 0.3, a typical value, then the reliability index decreases from 7.4 to 2.48 (for example, using FOSM) for Case 1 (m=0.6). Variability in soil unit weight and inclination of seismic force has relatively very low impact on the reliability index, as can be seen from Figure 6. Due to the combined effect of all the variables, the reliability index decreases considerably which affects the performance level of the slope under consideration. Thus, the COV of input variables has significant influence on the reliability index.

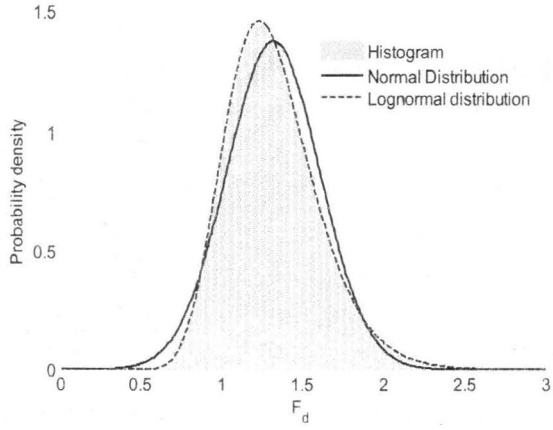

Fig. 5 Histogram and assumed normal and lognormal probability density functions of pseudo-static safety factor (Case 1)

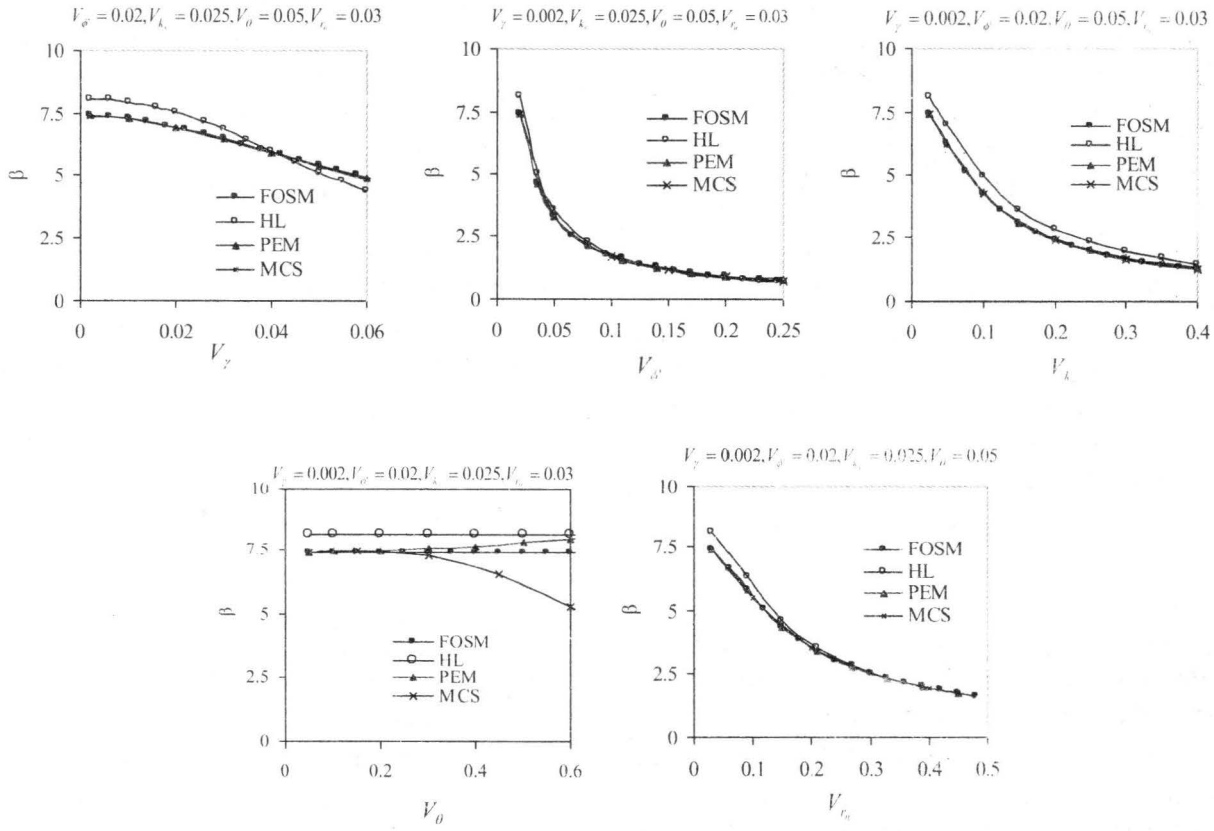

Fig. 6 Comparison of reliability index calculated by the FOSM, AFOSM (HL), PEM and MCSM

Table 1 Mean and COV of variables (F_d is the calculated deterministic safety factor)

Case	m	H	α	ϕ'	γ	k_s	θ	r_u	F_d
1	0.6	5 m	10°	35°	18	0.1	30°	0.2	1.278
2	0.2								1.75
COV (for both cases)				0.1	0.03	0.3	0.5	0.4	

Table 2 Reliability index using different methods

Case	m	β_{FOSM}	β_{HL}	β_{PEM}	β_{MCSM}
1	0.6	1.01	1.12	1.13	1.11
2	0.2	2.05	2.58	2.14	2.10

Mean and variance of excess pore pressure

As shown in Figure 6, variability in the excess pore pressure ratio significantly reduces the reliability index and it is necessary to determine the mean value and the COV of the excess pore pressure ratio. Excess pore pressure developed during seismic events at a specific instant can be evaluated from the empirical relationship proposed by Seed et al. (1975 a) as:

$$r_u = \frac{2}{\pi}\sin^{-1}\left[\left(\frac{N_{eq}}{N_{liq}}\right)^{\frac{1}{2\alpha}}\right] \qquad (25)$$

where N_{eq} is the equivalent number of uniform cycles representing earthquake motion, N_{liq} is the number of uniform cycles causing liquefaction or excess pore pressure ratios equal to one and α is an empirical constant. Both N_{liq} and α can be determined from stress controlled cyclic triaxial tests. For a given soil, N_{liq} is proportional to relative density and inversely proportional to the magnitude of loading; α depends on the soil type and test conditions. The lower and upper values of α as shown in Figure 7 are 0.5 and 0.9, respectively with a mean value of 0.7. N_{eq}, an equivalent number of uniform cycles during an earthquake depend on earthquake magnitude M. For a given magnitude of M, mean value of N_{eq} ($\mu_{N_{eq}}$) and N_{eq} at intervals of $\pm 1\sigma$ can be obtained from the empirical chart developed by Seed et al. (1975 b), shown in Figure 8. For an earthquake of magnitude, M = 7, $\mu_{N_{eq}}$ is 10, N_{eq} at $\pm 1\sigma$ are 15 and 5, respectively, and $\sigma_{N_{eq}}$ = (15-5)/2 = 5 and COV of N_{eq} ($V_{N_{eq}}$) = 5/10 = 0.5 (50%). Similarly, for an earthquake of magnitude, M = 7.5, $\mu_{N_{eq}}$ is 15, N_{eq} at $\pm 1\sigma$ are 23 and 8, respectively and thus $\sigma_{N_{eq}}$ = (23-8)/2 = 7.5 and COV of N_{eq} ($V_{N_{eq}}$) = 7.5/15 = 0.5 (50%).

Therefore a typical COV of N_{eq} may be assumed to be 0.5. The standard deviation of α (σ_α) can be calculated similarly, using the 3σ rule (Duncan 2000), as $\sigma_\alpha = (0.9-0.5)/6 \approx 0.07$ and COV as $V_\alpha = 0.07/0.7 = 0.1\ (10\%)$

Depending upon the variability of α and N_{eq}, the variability in r_u can be expressed by using FOSM as:

$$Var(r_u) = \left(\frac{\partial r_u}{\partial \alpha}\right)^2 Var(\alpha) + \left(\frac{\partial r_u}{\partial N_{eq}}\right)^2 Var(N_{eq}) \qquad (26)$$

where, $\partial r_u / \partial \alpha$ and $\partial r_u / \partial N_{eq}$ are the partial derivatives of r_u with respect to α and N_{eq}, respectively, evaluated at their mean values. Figure 9 shows the effect of COV of N_{eq} and a constant COV of α on the COV of excess pore pressure ratios for different values of N_{liq} (indirectly related to the soil relative density). The increase in COV of N_{eq} also increases the COV of r_u for a given N_{liq}. As N_{liq} increases, there may be either an increase or decrease in the COV of r_u depending upon the COV of N_{eq}. Similarly for a constant COV of N_{eq}, there is increase in the COV of r_u for an increasing COV of α and increasing N_{liq}. For a typical value of $V_{N_{eq}}$ =0.5 and V_α =0.1, $V_{r_u} \approx 0.39-0.42$ depending on $N_{liq} = 20-100$.

A typical value of $V_{r_u} = 0.4$ may be assumed appropriate for reliability evaluation of slopes considering variability in excess pore pressure ratio. Even though the other variables have negligible or minimum variability, variability in r_u is expected and this is attributed to model uncertainty (variability in α) and variability in N_{eq} during a seismic event. As shown in Figure 6, the reliability index (e.g. using FOSM) decreases from 7.4 to 1.91 if the variability in r_u (COV=0.4, COV of other variables as minimum) is considered for Case 1 (m = 0.6) and the reliability index decreases from 14.7 to 3.85 for Case 2 (m = 0.2).

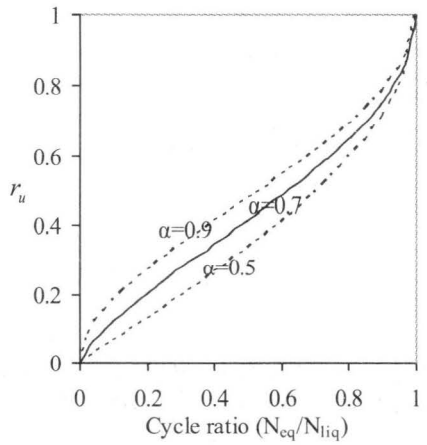

Fig. 7 Excess pore pressure generation as a function of cycle ratio (modified from Seed et al. 1975)

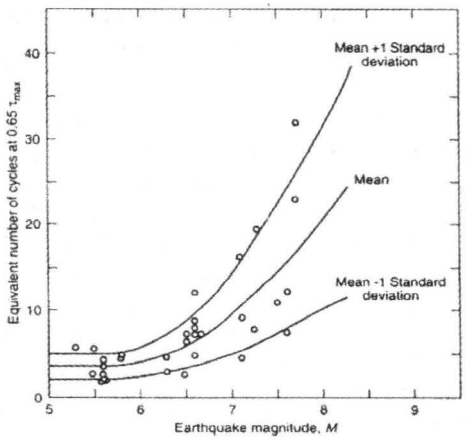

Fig. 8 Number of equivalent stress cycles N_{eq}, for different earthquake magnitudes (after Seed et al. 1975)

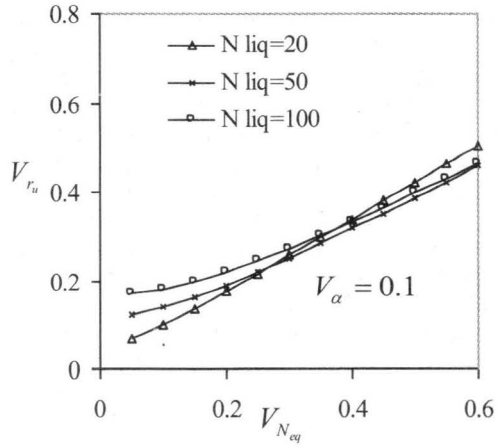

Fig 9a

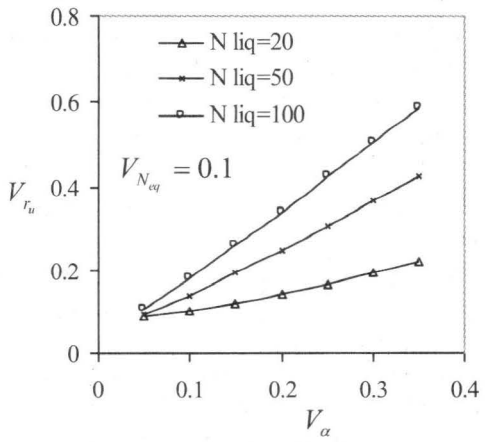

Fig 9b

Fig. 9 Effect of COV of N_{eq} and constant α on the COV of excess pore pressure ratio

Effect of parameters variability on permanent deformation

A displacement analysis of the slope can be carried out by double integrating the equation of motion expressed in Eq. 13, replacing k_c by k_{ch}. For a given earthquake input motion, the displacement is mainly dependent on k_{ch}. Eq. 13 requires a step-by-step numerical integration to calculate the dynamic displacements of the slope. Dividing the excitation time into a series of small increments, δt; by the linear acceleration method (Biggs 1964), the relative velocity $v(t + \delta t)$, and the displacement of the slide mass $d(t + \delta t)$, at time $t + \delta t$ can be calculated from the previous values, $v(t)$ and $d(t)$, at time t as

$$v(t+\delta t) = v(t) + \frac{a(t) + a(t+\delta t)}{2}\delta t \qquad (27a)$$

$$d(t+\delta t) = d(t) + v(t)\delta t + \frac{2a(t) + a(t+\delta t)}{6}\delta t^2 \qquad (27b)$$

The seismic record used in the analysis is shown in Figure 10 (adopted from the online strong motion database source: http://db.cosmos-eq.org). The strong motion data is taken from the site where the peak ground acceleration (PGA) is 0.604g (Takatori, Kobe 1995 earthquake, Japan). The displacements obtained for the strong motion using the simplified Newmark method are shown in Figure 11 for the infinite slope (Case 1). Here the value of k_{ch} has been assumed constant and its value was obtained as 0.150 using the mean value of all the parameters. A permanent displacement of 115 cm was obtained.

Due to uncertainties in soil and seismic parameters, k_{ch} will be a random variable. Assuming all the variables have normal distributions, the mean and COV of k_{ch} are found to be 0.1507 and 0.32, respectively. The histogram and the fitted normal and lognormal distributions of k_{ch} are shown in Figure 12. Figure 11 also shows the displacement obtained for $\mu \pm \sigma$ of k_{ch} where it can be found that the permanent displacements are 70 and 188 cm for $\mu + \sigma$ and $\mu - \sigma$ of k_{ch}, respectively. This suggests a high degree of uncertainty for the permanent displacement of the infinite slope. The uncertainty in the actual displacement of the infinite slope depends on both the variability of k_{ch} and the strong motion time history.

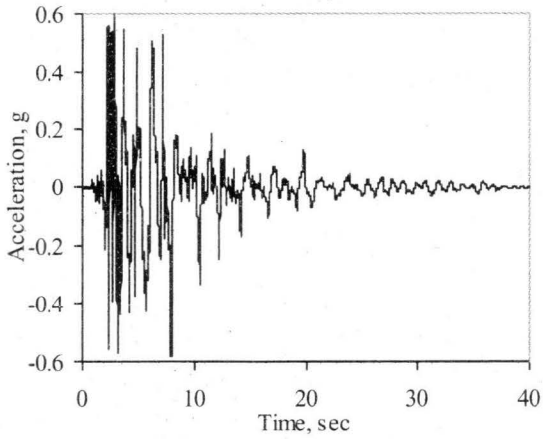

Fig. 10 Seismic record used in the analysis

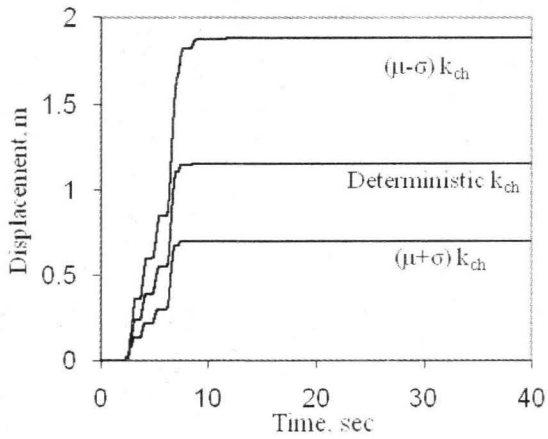

Fig. 11 Displacement calculation using the Newmark method

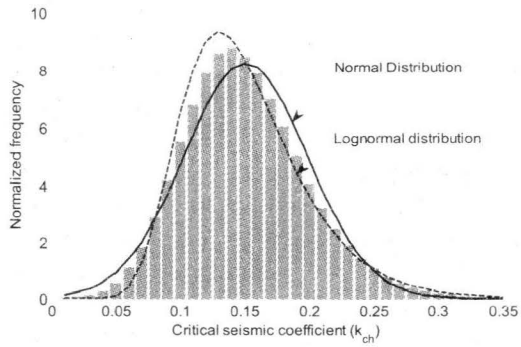

Fig. 12 Histogram and assumed probability density functions of the horizontal critical seismic coefficient

Conclusions

A reliability analysis of shallow landslides under seismic loading is performed using Infinite slope method and Newmark simplified block model. Based on deterministic and probabilistic analyses, the following conclusions are made:

Critical seismic coefficients obtained by assuming that the seismic force is either parallel to slope, horizontal or at a specific angle to the horizontal overestimate the critical seismic coefficient. The critical seismic coefficient should be determined assuming that the seismic force makes an angle $\phi' - \alpha$ with horizontal.

Due to high uncertainty associated with the determination of the excess pore pressure empirical model, the reliability index of infinite cohesionless slope is significantly reduced. A high variability in excess pore pressure is obtained due to variability in model constants and variability in the equivalent uniform stress cycle representation of an earthquake's magnitude. A typical COV of 0.4 is recommended for excess pore pressure ratio if Seed's excess pore pressure evaluation model is used.

For a given mean and COV of soil parameters, seismic parameters, excess pore pressure ratio, the reliability index of an infinite slope differs considerably depending on the probabilistic method used. Relative difference in computed reliability index using FOSM, AFOSM, PEM and MCSM is dependent on the soil variability, seismic parameters variability, as well as initial slope conditions. Though some difference in reliability index is obtained using different probabilistic methods, all these probabilistic methods consider the effect of uncertainty in soil and seismic parameters that are not accounted for in deterministic analysis. Thus, these probabilistic methods are recommended for shallow landslides analyses.

Acknowledgements

The Earthquake Engineering Research Center (EERC) at the University of California, Berkeley is gratefully acknowledged for permission to reproduce Figure 8.

References

Al-Homouda, A.S., Tahtamoni, W.W. (2000): Reliability analysis of three-dimensional dynamic slope stability and earthquake-induced permanent displacement by. . *Soil Dynamics and Earthquake Engg.*, 19, pp. 91-114.

Baecher, G. B. and Christian, J. T. (2003): *Reliability and statistics in geotechnical engineering*, John Wiley and Sons, New York, USA.

Baker, R., Shukha, R., Operstein, V. and Frydman, S. (2006): Stability charts for pseudo-static slope stability analysis. *Soil Dynamics and Earthquake Engg.*, 26, pp. 813-823.

Biggs, J. M. (1964): *Introduction to structural dynamics*. McGraw- Hill Book, New York.

Biondi, G., Cascone, E., Maugeri, M. and Motta, E. (2000): Seismic response of saturated cohesionless slopes. *Soil Dynamics and Earthquake Engg.*, 20, pp. 209-215.

Biondi, G., Cascone, E. and Maugeri, M. (2002): Flow and deformation failure of sandy slopes. *Soil Dynamics and Earthquake Engg.*, 22, pp. 1103-1114.

COSMOS Virtual Data Center (1999): http://db.cosmos-eq.org, the Consortium of Organizations for Strong-Motion Observation System (Date of access: 10.06.2009).

Duncan, J. M. (2000): Factors of safety and reliability in geotechnical engineering. *J Geotech Geoenviron Engg.*, 126(4), pp. 307-316.

Hasofer, A. M. and Lind, N. (1974): An exact and invariant first-order reliability format. *Journal of Engineering Mechanics*, 100(1), pp. 111-121.

Hassan A. M. and Wolff T. F. (2000): Effect of deterministic and probabilistic models on slope reliability index. *Slope stability 2000, GSP No. 101* (Eds. Griffiths, Fenton, and Martin), pp. 194-208

Hata, Y., Ichii, K., Tsuchida, T., Kano, S. and Yamashita, N. (2008): A practical method for identifying parameters in the seismic design of embankments. *Georisk: Assessment and Management of Risk for Engineered Systems and Geohazards*, 2(1), pp. 28 - 40.

Ingles, J., Darrozes, J., Soula, J. C. (2006): Effect of the vertical component of ground shaking on earthquake induced landslide displacements using generalized Newmark analysis. *Journal of Engg. Geology*, 86, pp. 134-147.

Kramer, S. L. and Lindwall, N. W. (2004): Dimensionality and directionality effects in Newmark sliding block analyses. *J. Geotech Geoenviron Engg.*, 130(3), pp. 303-315.

Kramer, S. L. (1996): *Geotechnical Earthquake Engineering*. NJ: Prentice Hall.

Low, B. K. and Tang, W. H. (1997): Efficient reliability evaluation using spreadsheet. *Journalof Engg. Mechanics*, 123(7), pp. 749-752.

Low, B. K. (2005): Reliability-based design applied to retaining walls. *Geotechnique*, 55(1), pp. 63-75.

Makdisi, F. I. and Seed, H. B. (1978): Simplified procedure for estimating dam and embankment earthquake induced deformations. *J Geotech Engg. Div. ASCE*, 104(7), pp. 849-867.

Malkawi, A. I. H., Hassan, W. F. and Abdulla, F. A. (2000): Uncertainty and reliability analysis applied to slope stability. *Structural Safety*, 22, pp. 161-187.

Newmark, N. M. (1965): Effect of earthquakes on dams and embankments. *Geotechnique*, 15(2), pp. 139-160.

Phoon, K. K. and Kulhawy, F. H. (1999): Characterization of geotechnical variability. Canadian Geotech Journal, 36, pp. 612-24.

Rosenblueth, E. (1975): Point estimates for probability moments. *Proc Natl Acad Sci USA*, 72(10), pp. 3812-3814.

Rosenblueth, E. (1981): Two point estimates in probabilities. *Appl Math Model*, 5, pp. 329-335.

Seed, H. B. and Goodman, R. E. (1964): Earthquake stability of slopes of cohesionless soils. *J Soil Mech Found Div-ASCE*, 90(6), pp.43-73.

Seed, H. B., Idriss, I. M., Makdisi, F. and Banerjee, N. (1975a): Representation of irregular stress time histories by equivalent uniform stress series in liquefaction analyses. *Report No EERC 75-29, Earthquake Engineering Research Centre*, University of California, Berkley.

Seed, H. B., Martin, P. P. and Lysmer, J. (1975b): The generation and dissipation of pore water pressures during soil liquefaction. *EERC 75-26, Earthquake Engineering Research Centre*, University of California, Berkeley.

Wang, K. L. and Lin, M. L. (2010): Development of shallow seismic landslide potential map based on Newmark's displacement: the case study of Chi-Chi earthquake, Taiwan. *Environmental Earth Science*, 60, pp. 775-785.

Xu, B. and Low, B. K. (2006): Probabilistic stability analyses of embankments based on finite element method. *J Geotech Geoenviron Engg.*, 132(11), pp. 1444-1454.